Pattern selection in oscillatory rotating convection

J. H. P. Dawes

Department of Applied Mathematics and Theoretical Physics, University of Cambridge, Silver Street, Cambridge, CB3 9EW, UK. Tel: +44-1223-337900. Fax: +44-1223-337918. Email: J.H.P.Dawes@damtp.cam.ac.uk

Abstract

Three-dimensional pattern selection in a low Prandtl number Boussinesq fluid with stress-free boundaries, where the onset of convection is oscillatory, is explored. Restricting the problem to a square lattice, the normal form coefficients are calculated as functions of τ (the square root of the Taylor number) and the Prandtl number σ. There is a large region of the (σ, τ) plane where a heteroclinic cycle connecting four Travelling Roll states is stable. As σ is decreased the cycle undergoes a transverse loss of stability, creating quasiperiodic orbits which may themselves become chaotic. All these stable dynamics occur at onset. Although conjectured on the basis of general results from symmetric bifurcation theory (and well-known for steady convection as the Küppers–Lortz instability [1]), cycling behaviour has not previously been demonstrated directly from the hydrodynamic equations in the oscillatory case. A second region of the (σ, τ) plane contains stable Travelling Roll solutions: we examine their stability to perturbations at varying angles and demonstrate the existence of small-angle instabilities of travelling rolls.

Key words: oscillatory convection, rotation, low Prandtl number, heteroclinic cycle.
PACS Codes: 47.54.+r; 47.20.Ky; 05.45.Ac

1 Introduction

It is well-known that the onset of convection in a rotating Boussinesq fluid with a low Prandtl number ($\sigma < 0.677$) is oscillatory if the rotation rate is large enough [3]; this criterion holds regardless of whether rigid or stress-free upper and lower boundary conditions are used. The nonlinear development of oscillatory convection has not been the subject of as much analysis as the steady case for which the Küppers-Lortz instability [1,4,5], and competing small-angle instabilities (for stress-free vertical boundaries) [2] have been identified.

Some aspects of the oscillatory instability have been previously analysed: in two dimensions Knobloch & Silber [6] analysed the relative stability of travelling and standing roll solutions for stress-free vertical boundaries. This work was extended to rigid vertical boundaries by Clune & Knobloch [7]. Riahi [8] analysed the linear stability of various standing roll planforms in two and three dimensions to general standing and travelling perturbations at a range of angles.

Most recently, Julien & Knobloch [12] have performed a three-dimensional asymptotic analysis in the limit of rapid rotation $\tau \to \infty$. In this limit the use of stress-free or rigid upper and lower boundary conditions becomes indistinguishable and degeneracies appear in the normal form equations describing the onset of convection. These degeneracies mean they could not determine the preferred planform of convection at high Taylor numbers. In section 4 we show how the results presented here for large τ agree with their analysis, and resolve the pattern selection problem. Although we use stress-free boundary conditions for computational convenience, we do not expect that the behaviour for large τ will qualitatively change if rigid boundaries are imposed in the vertical direction since the solution of the linear problem is insensitive to the choice of upper and lower boundary conditions [7,27].

The outline of the paper is as follows. In section 2 we specify the idealised convection problem considered, and derive the normal form equations. The results of the computations of the normal form coefficients are presented in Section 3. Section 4 considers the limit of rapid rotation, $\tau \to \infty$, and demonstrates that the results presented here agree with the analysis of Julien & Knobloch [12]. Section 5 considers the stability of travelling roll solutions to perturbations at oblique angles. Conclusions are drawn in section 6.

2 Rotating convection

Rotating Boussinesq convection is governed by three dimensionless parameters: the Prandtl number $\sigma = \nu/\kappa$ (the ratio of the rates at which velocity and temperature gradients diffuse), the Rayleigh number R which is proportional to the temperature difference across the layer and the square root of the Taylor number $\tau = 2\Omega h^2/\nu$ where h is the depth of the layer, Ω is the rotation rate and ν is the kinematic viscosity. We assume throughout the paper that the Boussinesq approximation holds [3]; fluid velocities are assumed to be much smaller than the sound speed, so the fluid can be treated as incompressible. Comparisons of the resulting linear theory (with rigid boundaries) have been seen to agree well with experimental results, even at large rotation rates ($\tau \sim 10^5$) [3] lending validity to the use of the Boussinesq equations over a wide region of parameter space. Let $\mathbf{u} = (u_x, u_y, u_z)$ and θ be pertur-

bations to the conduction solution $\mathbf{u}_0 = 0$, $T_0 = 1 - z$ (in a co-rotating frame) for the velocity and temperature fields respectively. The evolution of these perturbations is governed by the following non-dimensionalised equations:

$$(\partial_t - \sigma\nabla^2)\nabla^2\mathbf{u} + \sigma\tau\partial_z\boldsymbol{\omega} + \sigma R\mathbf{D}\,\theta = \nabla \times \nabla \times (\boldsymbol{\omega} \times \mathbf{u}), \tag{1}$$

$$(\partial_t - \nabla^2)\theta - u_z = -\mathbf{u} \cdot \nabla\theta, \tag{2}$$

$$\nabla \cdot \mathbf{u} = 0, \tag{3}$$

where the double curl of the momentum equation has been taken (to eliminate the modified pressure containing the centrifugal term), $\boldsymbol{\omega} = \nabla \times \mathbf{u}$ and the vector operator $\mathbf{D} \equiv (\partial^2_{xz}, \partial^2_{yz}, -\partial^2_{xx} - \partial^2_{yy})$. We impose periodic boundaries in the horizontal directions and stress-free, fixed temperature upper and lower boundaries:

$$\partial_z u_x = \partial_z u_y = u_z = \theta = 0 \qquad \text{at} \quad z = 0, 1. \tag{4}$$

From a linear stability analysis of the conduction (trivial) solution [3], the critical Rayleigh number for the onset of oscillatory convection at wavenumber α_o is found to be

$$R_o = \frac{2\sigma^2\pi^2\tau^2}{\alpha_o^2(1+\sigma)} + \frac{2(\alpha_o^2 + \pi^2)^3(\sigma + 1)}{\alpha_o^2}, \tag{5}$$

the corresponding frequency of the oscillations at onset is given by

$$\omega_0^2 = (\alpha_o^2 + \pi^2)^2\sigma^2\left[\frac{\tau^2\pi^2(1-\sigma)}{(\alpha_o^2 + \pi^2)^3(1+\sigma)} - 1\right]. \tag{6}$$

2.1 The normal form

By imposing a square lattice we reduce the symmetry group of the problem from the non-compact special Euclidean group $SE(2)$ of rotations and translations of the plane to the compact group $\mathbb{Z}_4 \ltimes T^2$. This ensures the existence of a finite dimensional centre manifold for the bifurcation problem. The problem of a Hopf bifurcation on a rotating square lattice has been analysed in detail by Knobloch & Silber [13] and their results are quoted in the next two sections. The fluid planform (as described by the vertical velocity for example) takes the form

$$\begin{aligned} u_z(x, y, z, t) = Re(&A_1 e^{\mathrm{i}(\alpha x - \omega_0 t)} + A_2 e^{-\mathrm{i}(\alpha x + \omega_0 t)} \\ &+ B_1 e^{\mathrm{i}(\alpha y - \omega_0 t)} + B_2 e^{-\mathrm{i}(\alpha y + \omega_0 t)}) f(z) \end{aligned} \tag{7}$$

where $f(z)$ represents the vertical structure of the solution. The amplitude equations $\dot{\mathbf{z}} = \mathbf{g}(\mathbf{z})$, $\mathbf{z} = (A_1, A_2, B_1, B_2)$, must be equivariant with respect to the group $\mathbb{Z}_4 \ltimes T^2 \times S^1$ generated by quarter-turn rotations about the z-axis and translations in the x and y directions and in time:

$$\begin{aligned} \rho : (x, y, t) &\to (y, -x, t) \\ (A_1, A_2, B_1, B_2) &\to (B_1, B_2, A_2, A_1) \end{aligned} \tag{8}$$

$$\begin{aligned} [(\xi, \eta), \phi] : (x, y, t) &\to (x + \xi/\alpha, y + \eta/\alpha, t + \phi/\omega_0) \\ (A_1, A_2, B_1, B_2) &\to (A_1 e^{\mathrm{i}\xi}, A_2 e^{-\mathrm{i}\xi}, B_1 e^{\mathrm{i}\eta}, B_2 e^{-\mathrm{i}\eta}) e^{-\mathrm{i}\phi} \end{aligned} \tag{9}$$

The time translation group S^1 is a normal form symmetry that occurs naturally for Hopf bifurcation problems. Thus the complete symmetry group of the problem is $\Gamma = \mathbb{Z}_4 \ltimes T^2 \times S^1$. Requiring equivariance with respect to these symmetries leads to the following system of ODEs (truncated at third order) for the four complex amplitudes:

$$\dot{A}_1 = A_1[\hat{\mu} + a|A_1|^2 + b|A_2|^2 + c|B_1|^2 + d|B_2|^2] + e\bar{A}_2 B_1 B_2 \tag{10}$$
$$\dot{A}_2 = A_2[\hat{\mu} + a|A_2|^2 + b|A_1|^2 + c|B_2|^2 + d|B_1|^2] + e\bar{A}_1 B_1 B_2 \tag{11}$$
$$\dot{B}_1 = B_1[\hat{\mu} + a|B_1|^2 + b|B_2|^2 + c|A_2|^2 + d|A_1|^2] + e\bar{B}_2 A_1 A_2 \tag{12}$$
$$\dot{B}_2 = B_2[\hat{\mu} + a|B_2|^2 + b|B_1|^2 + c|A_1|^2 + d|A_2|^2] + e\bar{B}_1 A_1 A_2 \tag{13}$$

where $\hat{\mu} = \mu + \mathrm{i}\tilde{\omega}(\mu)$ and both μ and $\tilde{\omega}$ are real. The coefficients a - e are also complex, in general. Since the normal form contains no quadratic terms, the bifurcation parameter μ can be scaled so that $|\mu|$=1; this implies there are no secondary bifurcations as μ increases from zero.

2.2 Primary branches

We recall the definitions of an isotropy subgroup $\Sigma_{\mathbf{z}} = \{\gamma \in \Gamma : \gamma\mathbf{z} = \mathbf{z}\}$ and a fixed point subspace $\mathrm{Fix}(\Sigma) = \{\mathbf{z} \in \mathbb{C}^4 : \gamma\mathbf{z} = \mathbf{z} \ \ \forall\ \gamma \in \Sigma\}$. The Hopf bifurcation with $\mathbb{Z}_4 \ltimes T^2$ symmetry generically produces four branches with two dimensional fixed point subspaces [13], which therefore exist for all values of the normal form coefficients by the Equivariant Hopf Theorem [14]. These are denoted Travelling Rolls (TR), Standing Rolls (SR), Standing Squares (SS) and Alternating Rolls (AR). A further periodic solution, Standing Cross Rolls (SCR), exists for some combinations of normal form coefficients - its existence is not guaranteed by the Equivariant Hopf Theorem since it has a four dimensional fixed point subspace. The stability properties of these periodic orbits depend on the values of the normal form coefficients a - e and

are summarised in table 1. Table 1 also contains a quasiperiodic solution, the Travelling Bimodal (TB) branch. This solution also has a four dimensional fixed point subspace and so is not guaranteed to exist for all coefficient values [13]. We expect that further doubly and triply-periodic solutions can exist in open regions of parameter space, as in the Hopf bifurcation with $D_4 \ltimes T^2$ symmetry [15].

2.3 The heteroclinic cycle

As noted by Knobloch & Silber [13], in an open region of the parameter space a structurally stable heteroclinic cycle exists and is asymptotically stable. In this section we summarise these existence and stability results. The existence of the heteroclinic cycle is directly related to the existence of the submaximal Travelling Bimodal (TB) solution. The invariant subspace $A_2 = B_2 = 0$ (equal to $\mathrm{Fix}(\Sigma_{TB})$) contains the two TR solutions $TR_1 = (A_1, 0, 0, 0)$ and $TR_2 = (0, 0, B_1, 0)$ corresponding to travelling rolls in the positive x-direction and the positive y-direction respectively and the TB solution $(r_1 e^{\mathrm{i}\omega_1 t}, 0, r_2 e^{\mathrm{i}\omega_2 t}, 0)$, where $r_1^2 = \mu(a_r - c_r)/(c_r d_r - a_r^2)$ and $r_2^2 = \mu(a_r - d_r)/(c_r d_r - a_r^2)$. The TB solution only exists when $a_r - c_r$ and $a_r - d_r$ have the same sign; from table 1 we see that the TB solutions appear when the Travelling Rolls lose or gain stability within this subspace: the TB solution coalesces with a TR fixed point as either $a_r - c_r \to 0$ or $a_r - d_r \to 0$. Within $\mathrm{Fix}(\Sigma_{TB})$ one of the TR solutions is a sink and the other is a saddle. As there are now no other invariant sets in $\mathrm{Fix}(\Sigma_{TB})$ there must be a saddle-sink connection between the two TR orbits for an open set of normal form coefficient values. The rotation symmetry ρ relating the behaviour near different TR orbits then forces the existence of a cycle connecting all four TR solutions, and this symmetry makes the stability properties of the cycle much easier to analyse. Asymptotic stability results for cycles between equilibria have been proved by Krupa & Melbourne [16]. These results also cover heteroclinic cycles connecting relative equilibria as is the case here [17,19]. The TR solution is a relative equilibrium because time evolution around the orbit is equivalent to the action of a spatial symmetry: for a point $\mathbf{z_0}$ on the orbit, $\phi_T(\mathbf{z_0}) = \gamma_T \mathbf{z_0}$ for some spatial translation γ_T which depends on T. This implies the existence of a continuous group orbit of TR solutions. None of the other four periodic solutions SR, SS, AR or SCR is a relative equilibrium.

The eigenvalues and corresponding eigenvectors for the TR_1 solution on the cycle can be labelled in the usual way [16,19] as *radial* (within $\mathrm{Fix}(\Sigma_{TR_1})$), *contracting* (in the B_2 direction), *expanding* (in the B_1 direction) and *transverse* (in the A_2 direction). In fact, the linearisation of (10) - (13) at a point on the TR_1 orbit, $D\mathbf{g}(\mathbf{z_0})$, is a diagonal matrix with entries which have non-zero real parts $\{-2\mu, \mu(1 - b_r/a_r), \mu(1 - d_r/a_r), \mu(1 - c_r/a_r)\}$; these are the radial,

transverse, expanding and contracting eigenvalues respectively. It is only these real parts that are important for the stability of the cycle, and fixing $\mu > 0$ and $a_r < 0$ so that the TR orbits bifurcate supercritically we consider the anticlockwise ($A_1 \to B_1 \to A_2 \to B_2 \to A_1$) case where

$$a_r - c_r > 0 \qquad \text{and} \qquad a_r - d_r < 0. \tag{14}$$

The symmetry ρ relating the four TR orbits implies that the stability of the cycle can be deduced from the dynamics near one TR orbit only. Necessary and sufficient conditions for asymptotic stability of this cycle are that the (real part of the) transverse eigenvalue to the cycle must be negative, and that the ratio of the absolute value of the real parts of the eigenvalues in the contracting and expanding directions must be greater than one. These conditions follow from a more general analysis of the stability of robust cycles [19], and here imply the following inequalities:

$$b_r - a_r < 0 \qquad \text{and} \qquad c_r + d_r - 2a_r < 0. \tag{15}$$

The inequalities (14) and (15) may be summarised as

$$\min(a_r - c_r, d_r - b_r, d_r - 2a_r) > d_r - a_r > 0 \tag{16}$$

which is a necessary and sufficient condition for asymptotic stability of the cycle. It is stronger than the sufficiency condition given in [13]: this latter result is derived directly from the sufficiency theorem of Melbourne et al. [20], and later theoretical work [18] has improved on this result.

3 Stable planforms on a square lattice

3.1 Periodic solutions

We calculate the normal form coefficients in (10) - (13) using modified perturbation theory, expanding the Rayleigh number R in powers of ε as well as the velocity and temperature fields:

$$(\mathbf{u}, \theta) = \varepsilon(\mathbf{u}_1, \theta_1) + \varepsilon^2(\mathbf{u}_2, \theta_2) + \dots \tag{17}$$

$$R = R_c + \varepsilon R_1 + \varepsilon^2 R_2 + \dots \tag{18}$$

We then equate the terms in (1) - (2) in each power of ε. This leads to the following schematic equations:

$$\mathcal{O}(\varepsilon): \quad \mathcal{L}(\mathbf{u}_1, \theta_1) = 0 \tag{19}$$
$$\mathcal{O}(\varepsilon^2): \quad \mathcal{L}(\mathbf{u}_2, \theta_2) = \mathcal{N}_1(\mathbf{u}_1, \theta_1) \tag{20}$$
$$\mathcal{O}(\varepsilon^3): \quad \mathcal{L}(\mathbf{u}_3, \theta_3) = \mathcal{N}_2(\mathbf{u}_1, \theta_1, \mathbf{u}_2, \theta_2) \tag{21}$$

where $\mathcal{L}$ is the linear operator on the LHS of equations (1) - (2) and $\mathcal{N}_1$ and $\mathcal{N}_2$ represent nonlinear terms. By taking stress-free, fixed temperature boundary conditions (4) the solution at each order can be expressed completely and simply in terms of exponentials. It would be possible to use a poloidal-toroidal decomposition, but the existence of mean flow terms means they would have to be explicitly added into the scheme. At $\mathcal{O}(\varepsilon^2)$ in the calculation there is a contribution from the term $\sigma R \mathbf{D}\,\theta$ containing R_1; by applying the solvability condition we find that $R_1 = 0$. At third order the values of the normal form coefficients are derived. The calculation was performed using the computer algebra package MAPLE. The algebraic expressions for the coefficients are far too large to give explicitly. Instead, the normal form coefficients were evaluated at a 26×40 grid of points in the (σ,τ)-plane: $0.025 \leq \sigma \leq 0.65$ in steps of 0.025 and for $25 \leq \tau \leq 1000$ in steps of 25. The stability of the primary branches discussed in section 2.2 was determined at each point, and stability boundaries in the (σ,τ) plane are indicated in figure 1.

The line ℓ_1 separates the regions where steady and oscillatory modes of convection are preferred at onset: above the line oscillatory convection is preferred. Line ℓ_2 where $a_r - b_r = 0$ was derived by Knobloch & Silber [6] since the required normal form coefficients can be calculated from the two-dimensional problem. It separates regions of stable TR and SR. Below ℓ_2 SR are stable. Above ℓ_2 TR are preferred, but may be unstable to perturbations in $\mathrm{Fix}(\Sigma_{TB})$. To the right of line ℓ_3 TR are stable to these perturbations and the quasiperiodic Travelling Bimodal solution exists (since $a_r - c_r$ and $a_r - d_r$ are both positive) but it is unstable. As ℓ_3 (the line given by $a_r - d_r = 0$) is crossed from right to left the TB solution disappears ($a_r - c_r$ is positive for all (σ, τ) and the product $(a_r - c_r)(a_r - d_r)$ is now negative). This leads to the formation of the stable robust heteroclinic cycle between all four TR states, as discussed in section 2.3. As indicated on figure 1, the stability criterion (16) for the cycle is satisfied to the left of ℓ_3, between ℓ_3 and ℓ_2.

3.2 Dynamics near the region of stable Standing Squares

The invariant subspace $\mathrm{Fix}(\Sigma_{SCR})$ (see table 1) defined by $A_1 = A_2 = A$ and $B_1 = B_2 = B$ contains the dynamics of a Hopf bifurcation with D_4 symmetry [21]. In the context of this problem (and also where it occurs in the Hopf bifurcation with $D_4 \ltimes T^2$ symmetry) it is called the SCR subspace since it is the fixed point subspace for the (submaximal) isotropy subgroup of the Standing Cross Rolls solution. It also contains the three periodic solutions

SR, SS and AR. The dynamics within the subspace are given by

$$A = A[\hat{\mu} + (a+b)|A|^2 + (c+d)|B|^2] + eB^2\bar{A} \tag{22}$$
$$B = B[\hat{\mu} + (a+b)|B|^2 + (c+d)|A|^2] + eA^2\bar{B} \tag{23}$$

As noted by Swift [21] there is a co-ordinate transformation which reduces the dimension of the dynamical equations to 2; the reduced equations were denoted the associated spherical system by Swift. Let $A = r^{1/2}e^{\mathrm{i}(\psi+\phi)/2}\cos\theta/2$, $B = r^{1/2}e^{\mathrm{i}(\psi-\phi)/2}\sin\theta/2$, then the evolution equations for θ and ϕ decouple after a time rescaling to remove the dependence on the 'radial' co-ordinate r:

$$\dot{\theta} = \sin\theta[\cos\theta(-f_r + e_r\cos 2\phi) - e_i\sin 2\phi] \tag{24}$$
$$\dot{\phi} = \cos\theta(f_i - e_i\cos 2\phi) - e_r\sin 2\phi \tag{25}$$

where $f = a + b - c - d$ and the subscripts r and i refer to real and imaginary parts respectively. We treat (θ, ϕ) as co-ordinates for latitude and longitude on the sphere. The periodic solutions in the SCR subspace are mapped to fixed points in the associated spherical system (24) - (25). Due to the periodicity of the trigonometric functions, we restrict the variables to $0 \leq \theta \leq \pi/2$ and $0 \leq \phi < \pi$ - half of the upper hemisphere in total. The SR solution is mapped to the 'North Pole' $\theta = 0$, the SS solution to $(\theta, \phi) = (\pi/2, 0)$ and the AR solution to $(\theta, \phi) = (\pi/2, \pi/2)$.

For the computed coefficients, it turns out that the AR solutions are never stable but there is a region of the (σ, τ) plane between ℓ_4 and ℓ_5 where the SS solutions are stable. There are two ways, generically, that the stability of the SS solution can change: the first is via a subcritical pitchfork bifurcation creating fixed points which correspond to the SCR periodic orbits. The second is via a Hopf bifurcation, creating a periodic orbit in (24) - (25) which corresponds to a quasiperiodic orbit in the normal form. The Hopf bifurcation from SS occurs across the line ℓ_4 in figure 1, and line ℓ_5 marks the pitchfork bifurcation. These lines meet at a codimension-2 point $\mathcal{C} = (\sigma^*, \tau^*)$ in figure 1. Near this point in parameter space it is possible to reduce the dynamics (24) - (25) around the SS fixed point to the normal form for a Takens-Bogdanov bifurcation with $\mathbb{Z}_2$ symmetry [30,29,28]. This proves the existence of a curve of global bifurcations emanating from $\mathcal{C}$ and completes the bifurcation diagram near $\mathcal{C}$, see figure 2. The remainder of this section summarises the reduction of the dynamics to the Takens-Bogdanov normal form.

The Hopf bifurcation from SS occurs when $f_r - 3e_r = 0$ and the pitchfork bifurcation occurs when $Re(f\bar{e}) - |e|^2 = 0$. Near the point $(\pi/2, 0)$ we write $\theta = \tilde{\theta} + \pi/2$ and $\phi = \tilde{\phi}$ and expand the sines and cosines in power series, truncating at cubic order. Dropping tildes we find:

$$\dot{\theta} = \theta(f_r - e_r) - 2e_i\phi + \frac{2}{3}\theta^3(e_r - f_r) + 2\theta\phi^2 e_r + (\frac{4}{3}\phi^3 + \theta^2\phi)e_i + \mathcal{O}(4), \quad (26)$$

$$\dot{\phi} = \theta(e_i - f_i) - 2e_r\phi + \frac{1}{6}\theta^3(f_i - e_i) - 2\theta\phi^2 e_i + \frac{4}{3}\phi^3 e_i + \mathcal{O}(4), \quad (27)$$

where $\mathcal{O}(4)$ denotes terms of degree 4 or higher in θ and ϕ. Now we rescale $(\theta, \phi) \to (\theta e_i, \phi e_r)$ and eliminate the constants f_r and f_i by moving to the codimension 2 point in parameter space: set $f_r = 3e_r$ and $f_i = (|e|^2 - 3e_r^2)/e_i$. We use successive transformations to put the equations in normal form. First we eliminate all but one of the linear terms by the linear change of variables $(u, v) = (\theta + \phi, \theta - \phi)$. The resulting equations for $\dot{u}$ and $\dot{v}$ have a linearisation with two zero eigenvalues, and a symmetry $(u, v) \to (-u, -v)$. By a near-identity transformation $(u, v) \to (x, y)$ we are able to remove all but two of the cubic terms in the $(\dot{u}, \dot{v})$ equations and are left with the following normal form for the Takens-Bogdanov bifurcation:

$$\dot{x} = y, \quad (28)$$

$$\dot{y} = \kappa y - \lambda x + P_1 x^3 + P_2 x^2 y, \quad (29)$$

where κ and λ are unfolding parameters, and $P_1 = e_r|e|^2/4$ and $P_2 = (7e_r^2 - 4e_i^2 - 4e_r^3 - 8e_i^2 e_r)/16$. At the point $\mathcal{C} = (\sigma^*, \tau^*)$ the numerical value of the coefficient e implies $P_1 > 0$ and $P_2 < 0$. This case of the Takens-Bogdanov bifurcation has been previously studied in connection with thermosolutal convection [22,28]. The normal form (28)-(29) correctly describes the behaviour in the SCR subspace close to the codimension-2 point $\mathcal{C}$. In particular there is a subcritical pitchfork bifurcation when $\lambda = 0$ and a supercritical Hopf bifurcation when $\kappa = 0$ and $\lambda > 0$. There is also a line of global bifurcations at $\kappa \simeq -\lambda P_2/5$ where the periodic orbit collides with the SCR fixed points, corresponding to the dashed line starting from $\mathcal{C}$ in figure 1. Along a line of constant $\tau > \tau^*$, see figure 2, exactly this behaviour is seen. This reduction to a normal form also proves the uniqueness of the quasiperiodic orbit for (22)-(23) near the codimension 2 point in parameter space where $f_r = 3e_r$ and $f_i = (|e|^2 - 3e_r^2)/e_i$. In passing we remark that uniqueness of the quasiperiodic orbit has also been proved in a neighbourhood of another point in the parameter space for (22) - (23) by van Gils & Silber [32]. The 'bubble' of stable SS solutions closes as the lines ℓ_4 and ℓ_5 cross over again at larger τ. The analysis of this second Takens-Bogdanov bifurcation is very similar to the first and so will not be discussed further.

3.3 Transverse bifurcation from the heteroclinic cycle

For $0.05 < \sigma < 0.2$, numerical simulations indicate the presence of other quasiperiodic solutions, outside the SCR subspace, see figure 3. These lie close

to the robust cycle discussed in section 2.3, but they are clearly distinct from it and stable. For some parameter values, at lower σ, triply-periodic and chaotic solutions appear, see figure 4. In these figures note that the value of μ affects the solutions only by scaling mode amplitudes by a constant factor. The creation of these quasiperiodic and chaotic solutions can be explained by the loss of stability of the heteroclinic cycle as σ decreases across ℓ_2. There are two ways in which robust heteroclinic cycles generically lose stability: either through resonant bifurcations where the ratio of the (real parts of the) contracting and expanding eigenvalues passes through 1, or through transverse bifurcations corresponding to eigenvalues in directions normal to the cycle crossing the imaginary axis. Here we find that the cycle undergoes a transverse bifurcation at ℓ_2. In this section we examine the dynamics near ℓ_2 in detail.

The analysis of [18] can be applied to this cycle because (as discussed in section 2.3) although the cycle is between periodic orbits, not equilibria, the TR solutions are relative equilibria. The fact that we do not explicitly need all the phases of the four amplitudes is brought out by a transformation of the normal form equations (10) - (13) to modulus and argument form. By writing $A_1 = r_1 e^{\mathrm{i}\theta_1}$, $A_2 = r_2 e^{\mathrm{i}\theta_2}$, $B_1 = r_3 e^{\mathrm{i}\theta_3}$, $B_2 = r_4 e^{\mathrm{i}\theta_4}$ we derive equations for the moduli r_j. We define $\psi = \theta_4 + \theta_3 - \theta_2 - \theta_1$:

$$\dot{r}_1 = r_1\left[\mu + a_r r_1^2 + b_r r_2^2 + c_r r_3^2 + d_r r_4^2\right] + e_+ r_2 r_3 r_4 \tag{30}$$

$$\dot{r}_2 = r_2\left[\mu + a_r r_2^2 + b_r r_1^2 + c_r r_4^2 + d_r r_3^2\right] + e_+ r_1 r_3 r_4 \tag{31}$$

$$\dot{r}_3 = r_3\left[\mu + a_r r_3^2 + b_r r_4^2 + c_r r_2^2 + d_r r_1^2\right] + e_- r_1 r_2 r_4 \tag{32}$$

$$\dot{r}_4 = r_4\left[\mu + a_r r_4^2 + b_r r_3^2 + c_r r_1^2 + d_r r_2^2\right] + e_- r_1 r_2 r_3 \tag{33}$$

$$\dot{\psi} = \Psi(r_1, r_2, r_3, r_4, \psi) \tag{34}$$

where $e_\pm = e_r \cos\psi \mp e_i \sin\psi$. In this reduction we can fix $\psi = 0$ whenever one of the r_j is zero since it is then undefined. As the heteroclinic cycle is contained entirely within subspaces where two of the r_j are zero, we can take $\psi = 0$ around the complete cycle.

Consider the $TR_1 = (A_1, 0, 0, 0)$ orbit. The heteroclinic connections into and out of TR_1 are contained in the two subspaces $TR_{in} = \{(A_1, 0, 0, B_2)\}$ and $TR_{out} = \{(A_1, 0, B_1, 0)\} = \mathrm{Fix}(\Sigma_{TB})$ (see table 1). The bifurcation is said to be *transverse* because the eigenvector corresponding to the eigenvalue $1 - b_r/a_r = 0$ in (30)-(34) is in the A_2-direction which is not contained in the subspace $Q = TR_{in} + TR_{out} = \{(A_1, 0, B_1, B_2)\}$. Chossat et al. [18] classify heteroclinic cycles into three types, referred to as A, B and C, depending on whether Q is a fixed-point subspace for some symmetry element $\gamma \in \Gamma$. A cycle is of type A if Q is not a fixed-point subspace for any γ; it is of type B if Q is a

fixed-point subspace for some γ and the entire cycle $X \subset Q$. It is of type C if Q is a fixed-point subspace for some γ but X does not lie completely within Q. Cycles of all three types occur naturally in systems with symmetry, and transverse bifurcations from each type are studied in [18]. The different cycle types give rise to different transverse bifurcation phenomena so the group theoretic distinction between them is crucial.

As a subspace which is not flow-invariant cannot be a fixed-point subspace for an element $\gamma \in \Gamma$, the subspace Q cannot be a fixed-point subspace (due to the form of the last term on the RHS of equations (30) - (33)) and so the cycle X under consideration is of type A. Chossat et al. prove [18, theorem 4.1] that when an equilibrium on a type A cycle undergoes a non-degenerate (supercritical) pitchfork bifurcation, and hence the transverse eigenvalue becomes positive, the cycle itself undergoes either a subcritical or a supercritical global bifurcation. This bifurcation creates a unique nearby stable or unstable periodic orbit close to the cycle. The bifurcation is termed 'flat' because the distance between the cycle and the periodic orbit varies as $|\Delta|^{1/\lambda}$ to leading order where Δ is a constant which depends only on the global part of the flow between the equilibria, and λ is the bifurcation parameter. If $|\Delta| < 1$ the periodic orbit is created supercritically and it is stable; if $|\Delta| > 1$ the periodic orbit is created subcritically and it is unstable. What is remarkable is that the direction of branching of the pitchfork bifurcation of the equilibria on the cycle is independent of the direction of branching of the 'flat' bifurcation of the cycle. Indeed, one is a purely local phenomenon and the other is determined only by the dynamics on the sections of the cycle not close to the equilibria.

The cycle between TR relative equilibria does not, as it stands, satisfy the conditions of [18, theorem 4.1] because the local bifurcation which transfers stability between TR and SR when $a_r - b_r = 0$ is degenerate for the cubic truncation we have so far considered, see [23] and [14, chapter XVII]. The 'pitchfork' bifurcation at $a_r - b_r = 0$ does not create any new small amplitude solutions near the TR orbits. Possible behaviours near this degeneracy have been classified completely by [34,35]; the degeneracy is unfolded by the addition of small perturbations in the form of fifth and seventh order terms to (30) - (34). When these higher-order terms are introduced into the normal form, stability is transferred between TR and SR via a branch of Modulated Travelling Rolls (MTR) which may itself be stable or unstable, see figure 5(a) and (b). The stability of the MTR branch does not affect the global bifurcation creating the periodic orbit in (30) - (34) as the stability of the periodic orbit depends on the global quantity Δ which is not affected at leading order by these fifth and seventh order terms. To calculate Δ we integrate the variational equation around the cycle and compute the eigenvalues of the resulting matrix. Since the four equilibria are related by symmetry it is enough to integrate the equations for $r_1 \ldots r_4$ around one quarter of the cycle: for example within $\mathrm{Fix}(\Sigma_{TB})$. Let the variational equation for (30) - (33) be $\dot{\Phi} = DF(\mathbf{z}(t))\Phi$. The

integration along the heteroclinic cycle is for a time interval $[0, T]$ defined by the initial conditions $\Phi(\mathbf{z}(0)) = I$ and $r_3(0) = \delta$, $r_1^2(0) = -\mu/a_r$, $|\delta| \ll 1$ and the final condition $r_1(t) = \delta$. The matrix DF is block-diagonal and the evolution of the (r_2, r_4)-variables is independent of that of the (r_1, r_3) variables. Since we are interested in the transverse (r_2) direction, it is enough to integrate the 2×2 sub-system in the r_2 and r_4 variables:

$$\dot{M} = \begin{pmatrix} DF_{22} & DF_{24} \\ DF_{42} & DF_{44} \end{pmatrix} M = \begin{pmatrix} \mu + b_r r_1^2 + d_r r_3^2 & e_r r_1 r_3 \\ e_r r_1 r_3 & \mu + b_r r_3^2 + c_r r_1^2 \end{pmatrix} M, \qquad (35)$$

with initial condition $M(\mathbf{z}(0)) = I$. Illustrative coefficient values are $a_r = -0.44348$, $b_r = -0.43842$, $c_r = -6.5616$, $d_r = 3.566$, $e_r = -0.12137$ for $(\sigma, \tau) = (0.075, 700)$ (very close to the line ℓ_2). Numerical integrations show that the matrix M has a positive eigenvalue greater than 1 in the r_2 (transverse) direction and a positive eigenvalue less than 1 in the r_4 direction. The exact values of these eigenvalues depend on the choice of δ but there is an $\mathcal{O}(1)$ contribution from the global portion of the trajectory which dominates $\mathcal{O}(\delta)$ contributions from near the TR equilibria. Thus an unstable periodic orbit bifurcates subcritically from the cycle at line ℓ_2 in figure 1. This periodic orbit for equations (30) - (34) appears as a quasiperiodic orbit for the normal form (10) - (13). For fixed $a_r < 0$, the bifurcation would become supercritical if d_r decreased far enough towards zero. However, numerical calculations show that in the (σ, τ) plane the coefficients do not vary enough for this to occur, and the transverse bifurcation is always subcritical; $|\Delta| > 1$ over the whole of the line ℓ_2 to the left of ℓ_3.

We conjecture that the existence of stable quasiperiodic solutions close to the transverse loss of stability of the cycle is due to the branch of subcritical quasiperiodic solutions turning around in a saddle-node bifurcation and giving rise to stable quasiperiodic orbits as indicated in figure 5(c). The very slow separation of the unstable orbit and the cycle means that the stable (quasiperiodic) orbit will remain closer to the cycle it coexists with than we might expect. As we continue to decrease σ at fixed τ the quasiperiodic orbit undergoes a bifurcation to a three-torus and then breaks up and becomes chaotic (see figure 4) for the values of τ indicated on figure 1.

4 Asymptotic behaviour as $\tau \to \infty$

Following the ideas of Bassom & Zhang [11], Julien & Knobloch [12] performed a weakly nonlinear analysis in the limit $\tau \to \infty$ by scaling (1) - (3) and applying modified perturbation theory to the resulting leading order equations.

From the point of view of planform selection this limit is very degenerate: at leading order the scaled equations have an unexpected reflection symmetry which introduces another primary solution branch, and forces $a = b$, $c = d$ and $e = 2a - 2c$ in the amplitude equations (10) - (13). This highly degenerate situation means that Julien & Knobloch were unable to give complete results for planform selection. To determine pattern selection at high τ either the asymptotic analysis of [12] must be carried out to include higher order terms or the normal form coefficients must be calculated directly. The results of direct calculations show that TR are the preferred mode of convection on a square lattice at high τ for all σ, agreeing with the partial conclusions of [12]. The modified perturbation theory discussed in section 3.1 produces coefficients which differ by a common scaling (in effect, a different choice of normalisation) from those given in the rapidly rotating limit by Julien & Knobloch. Ratios of coefficients are unaffected by this scaling, and so should agree for the two calculations. The convergence of the ratio a_r/c_r in the limit $\tau \to \infty$ is demonstrated in figure 6 and agrees very well with the results of [12].

Clune & Knobloch [7] estimated that the behaviour for $\tau > 10^6$ should agree well with asymptotic results. We find that this holds for moderate σ, but for $\sigma \ll 0.1$ the true asymptotic regime is not reached until τ is substantially higher, say $\tau \simeq 10^{10}$. Hence calculations at finite, but large, τ may not correctly model the asymptotic regime for small σ. This indicates the possible relevance of distinguished limits of small σ and rapid rotation: fix $\sigma\tau^{1/n} = s$ where s is $\mathcal{O}(1)$ and $n \geq 1$, but let $\tau \to \infty$ so that $\sigma \to 0$ at the same time. The case $n = 1$ has been considered by Zhang & Roberts [9], and Bassom & Zhang [10] and produces convective modes they term 'thermal-inertial' waves. As we consider limits with larger and larger n we might expect the dynamics in the distinguished limit to approach those in the simpler limit $\tau \to \infty$, $\sigma \sim 1$ analysed by [12]. Further work on this problem is in progress [27].

5 Stability to perturbations off the lattice

By restricting the problem to a square lattice in earlier sections we can only investigate the stability of TR to perturbations at multiples of 90°. In a spatially extended layer of fluid there may well be instabilities of TR to perturbations at other angles. This is well-known for steady rolls, demonstrated first by Küppers & Lortz [1] who showed, in the limit of infinite Prandtl number, that the maximum growth rate of an instability of steady rolls was obtained to rolls aligned at $\simeq 58°$ to the original rolls and the instability occurred as long as $\tau^2 > 2285$. Calculations at finite σ have been reported by Clune & Knobloch in [7]. More recently, Cox & Matthews [2] have completed the study of small-angle instabilities of steady rolls when stress-free vertical boundaries are used.

For a fixed angle Θ we examine the stability of TR to perturbations oriented at a finite angle by imposing a rhombic lattice generated by vectors $\mathbf{k_1} = (1, 0)$ and $\mathbf{k_2} = (-\cos\Theta, \sin\Theta)$, see figure 7(a), instead of a square one. The fluid planform is now

$$u_z(x,y,z,t) = Re(A_1 e^{\mathrm{i}(\alpha \mathbf{k_1}\cdot\mathbf{x}-\omega_0 t)} + A_2 e^{-\mathrm{i}(\alpha \mathbf{k_1}\cdot\mathbf{x}+\omega_0 t)} + B_1 e^{\mathrm{i}(\alpha \mathbf{k_2}\cdot\mathbf{x}-\omega_0 t)} + B_2 e^{-\mathrm{i}(\alpha \mathbf{k_2}\cdot\mathbf{x}+\omega_0 t)}) f(z) \tag{36}$$

The symmetry group of this planform is $\mathbb{Z}_2 \ltimes T^2 \times S^1$ - the only rotational symmetry is a half-turn ρ^2. However, the amplitude equations are required to be equivariant with respect to additional 'hidden' symmetries inherited from the $SE(2)$ equivariance of the original problem [31]; they now take the form

$$\dot{A}_1 = A_1[\hat{\mu} + a|A_1|^2 + b|A_2|^2 + c|B_1|^2 + d|B_2|^2] + e\bar{A}_2 B_1 B_2 \tag{37}$$
$$\dot{A}_2 = A_2[\hat{\mu} + a|A_2|^2 + b|A_1|^2 + c|B_2|^2 + d|B_1|^2] + e\bar{A}_1 B_1 B_2 \tag{38}$$
$$\dot{B}_1 = B_1[\hat{\mu} + a|B_1|^2 + b|B_2|^2 + \tilde{c}|A_2|^2 + \tilde{d}|A_1|^2] + \tilde{e}\bar{B}_2 A_1 A_2 \tag{39}$$
$$\dot{B}_2 = B_2[\hat{\mu} + a|B_2|^2 + b|B_1|^2 + \tilde{c}|A_1|^2 + \tilde{d}|A_2|^2] + \tilde{e}\bar{B}_1 A_1 A_2 \tag{40}$$

where the complex coefficients $a, b, c, d, e, \tilde{c}, \tilde{d}, \tilde{e}$ depend on the lattice angle Θ. The stability of a (for example) $(0, 0, B_2, 0)$ solution to perturbations in the A_1 mode changes when $a_r - d_r = 0$ exactly as in the square lattice case: there is a Travelling Bimodal solution in the $A_2 = B_1 = 0$ subspace which exists as long as $a_r - d_r$ and $a_r - \tilde{c}_r$ have the same sign. To compute the stability of TR to perturbations at an angle Θ we evaluate the coefficient d_r as Θ varies. These stability calculations show that the region of stable TR shrinks as Θ decreases: figure 8 shows the lines $a_r - d_r(\Theta) = 0$ for $\Theta = 40°, 50°, 60°, 70°$ and $80°$. TR are stable to these perturbations to the right of these lines. Note that ℓ_3 corresponds to $\Theta = 90°$. As $\Theta \to 0$ the growth rates of the instability appear to grow unboundedly, see figure 7(b). This is due to the resonant interaction of the two modes $e^{\mathrm{i}(\alpha \mathbf{k_1}\cdot\mathbf{x}-\omega_0 t)}$ and $e^{-\mathrm{i}(\alpha \mathbf{k_2}\cdot\mathbf{x}+\omega_0 t)}$ as in steady rotating convection [2]. At $\mathcal{O}(\varepsilon^2)$ in the modified perturbation calculation we find contributions to the u_x solution which, in the limit as $\Theta \to 0$ at fixed ε asymptote as

$$u_x \sim \frac{\varepsilon^2}{\Theta} A_1 \bar{B}_2 e^{\mathrm{i}\alpha[(1-\cos\Theta)x - y\sin\Theta]} \tag{41}$$

indicating a breakdown in the scalings adopted in the analysis in the limit of small Θ. Terms such as this one cause the coefficient $d_r(\Theta)$ to blow up at small angles. If $d_r(\Theta) \gg 1$ for small angles then small-angle perturbations will grow; if $d_r(\Theta)$ becomes large but negative then the TR are increasingly stable to perturbations in the small-angle limit and this blow up does not generate an instability. A similar analysis to that performed by Cox & Matthews

[2] should be possible to analyse this small-angle instability which may dominate the observed behaviour in spatially-extended systems with stress-free boundaries. It is likely that employing rigid boundaries would damp the resulting mean flows and so remove these instabilities. Comparing the variation of the coefficient $d_r(\Theta)$ in figure 7(b) to [7, figure 12] (which is calculated for $\sigma = 100$) we see that the 'boundary-layer' behaviour of the coefficient is apparent for $\Theta \leq 10^\circ$ in both cases, but in the steady case the original rolls are stable to perturbations at angles just outside the 'boundary-layer', whereas here perturbations with $\Theta \simeq 10^\circ$ to the original travelling rolls will grow with an order 1 growth rate, and the smaller the angle, the larger the growth rates of perturbations become. Because of this, even if rigid boundaries resolved the blow up of the growth rates for small Θ by making the growth rates tend to a finite (positive) value in the limit $\Theta \to 0$, we would still expect TR to be unstable to perturbations at a range of small angles. Since the relevant calculations with rigid boundaries have not yet been carried out this remains conjectural. Calculations of the stability of TR in limits of rapid rotation and small σ, where rigid and stress-free boundaries are indistinguishable, also show a small-angle instability [27]. This is in sharp contrast to the behaviour noted above for steady rolls, where the use of rigid boundaries stabilises rolls to all perturbations below a critical (order 1) angle.

6 Discussion and conclusions

We have analysed weakly nonlinear three-dimensional rotating convection with a square planform for all values of the Prandtl and Taylor numbers. This analysis shows the existence of a structurally stable heteroclinic cycle, quasiperiodic, and chaotic behaviour in the resulting amplitude equations. This analysis, although complete in itself, has several limitations. Most importantly, although we have done as much as is possible, the theory does not yet allow for a full discussion of the stability of our solutions to modes at varying angles. We have also not discussed modulational instabilities, either to finite wavelength perturbations, as discussed for steady hexagonal patterns by Echebarria & Riecke [33], or those on asymptotically long lengthscales.

We have seen that although TR are the preferred planform for a large region of the (σ, τ) plane for modes restricted to a square lattice, they are unstable to perturbations at smaller angles in the anticlockwise (co-rotating) direction. Likewise, the quasiperiodic solutions in the normal form may also not be stable to these perturbations. This analysis has, however, indicated the strong possibility of heteroclinic cycles, quasiperiodic and chaotic behaviour at onset even in small aspect ratio systems. All our calculations have been carried out with stress-free vertical boundaries for computational convenience. We hope that qualitative features of the dynamics will persist for rigid boundaries,

probably shifted to higher Taylor numbers as has been shown to happen for the line ℓ_2 [7]. We remark that the results of sections 3, 4 and 5 do not depend critically on the Boussinesq symmetry of the PDEs since even in its absence the normal forms for the Hopf bifurcations will not contain quadratic terms.

In the limit of rapid rotation our results agree quantitatively with those of Julien & Knobloch [12]. The line ℓ_3 seems, for large τ, to asymptote towards a curve of the form $\sigma^4\tau = \text{const}$. The significance of this relationship between σ and τ is examined in detail in [27].

We have not investigated further the stability of the SR: Riahi [8] has previously calculated that SR are unstable to perturbations at angles less than 90°. In a spatially extended system we may expect complex dynamics in the region where SR are stable in figure 1 for the $\mathbb{Z}_4 \ltimes T^2$-symmetric normal form: either cycling behaviour between sets of SR at different orientations as discussed by Knobloch & Silber [31] or chaotic behaviour associated with the Shil'nikov dynamics investigated by Swift & Barany [24] for SR on a rotating hexagonal lattice.

The nonlinear development of the small-angle instability identified in section 5 and the extent to which these instabilities persist for oscillatory convection with rigid boundaries are subjects which it would be of interest to pursue further. It should be possible to perform a detailed analysis of the small-angle instability in a similar way to that already done in the steady case [2], but if the instability does not persist when rigid boundaries are used it is probably of limited physical significance.

Experiments using liquid metals such as mercury and gallium, and mixtures of cooled and pressurised gases [25] have resulted in a large number of quantitative measurements of pattern-formation phenomena in convection at low Prandtl numbers, and it would be of great interest to compare the results of experiments conducted in the oscillatory regime with the dynamics explored in this paper.

Acknowledgements

I have benefited from discussions with Michael Proctor and Alastair Rucklidge. The presentation of this work has been greatly improved by many perceptive and helpful comments from two anonymous referees. This work was funded by the UK EPSRC.

References

[1] G. Küppers and D. Lortz, Transition from laminar convection to thermal turbulence in a rotating fluid layer. *J. Fluid Mech.* **35** 609–620 (1969)

[2] S.M. Cox and P.C. Matthews, Instabilities of rotating convection. *J. Fluid Mech.* **403** 153–172 (2000)

[3] S. Chandrasekhar, *Hydrodynamic and Hydromagnetic Stability.* Oxford University Press (1961), republished by Dover Publications, Inc. (1981)

[4] R.M. Clever and F.H. Busse, Nonlinear properties of convection rolls in a horizontal layer rotating about a vertical axis. *J. Fluid Mech.* **94** 609–627 (1979)

[5] F.H. Busse and K.E. Heikes, Convection in a rotating layer. *Science* **208** 173–175 (1980)

[6] E. Knobloch and M. Silber, Travelling wave convection in a rotating layer. *Geophys. Astrophys. Fluid Dynamics.* **51** 195–209 (1990)

[7] T. Clune and E. Knobloch, Pattern selection in rotating convection with experimental boundary conditions. *Phys. Rev.* E **47** 2536–2550 (1993)

[8] D.N. Riahi, Weakly nonlinear oscillatory convection in a rotating fluid. *Proc. R. Soc. Lond.* A **436** 33–54 (1992)

[9] K. Zhang and P.H. Roberts, Thermal inertial waves in a rotating fluid layer: exact and symptotic solutions. *Phys. Fluids* **9** 1980–1987 (1997)

[10] A.P. Bassom and K. Zhang, Finite amplitude thermal inertial waves in a rotating fluid layer. *Geophys. Astrophys. Fluid Dynamics* **87** 193–214 (1998)

[11] A.P. Bassom and K. Zhang, Strongly nonlinear convection cells in a rapidly rotating fluid layer. *Geophys. Astrophys. Fluid Dynamics* **76** 223–238 (1994)

[12] K. Julien and E. Knobloch, Fully nonlinear three-dimensional convection in a rapidly rotating layer. *Phys. Fluids* **11** 1469–1483 (1999)

[13] E. Knobloch and M. Silber, Hopf Bifurcation with $\mathbb{Z}_4 \times T^2$ Symmetry. *Int. Series of Numer. Math.* **104** 241–252 (1992)

[14] M. Golubitsky, I.N. Stewart and D.G. Schaeffer, *Singularities and Groups in Bifurcation Theory. Volume II.* Springer, Applied Mathematical Sciences Series **69** (1988).

[15] J.H.P. Dawes, Stable quasiperiodic solutions in the Hopf bifurcation with $D_4 \ltimes T^2$ symmetry. *Physics Letters* A **262** 158–165 (1999)

[16] M. Krupa and I. Melbourne, Asymptotic stability of heteroclinic cycles in systems with symmetry. *Ergod. Th. & Dynam. Sys.* **15** 121–147 (1995)

[17] M. Krupa, Bifurcations of relative equilibria. *SIAM J. Appl. Math.* **21** 1453–1486 (1990)

[18] P. Chossat, M. Krupa, I. Melbourne and A. Scheel, Transverse bifurcations of homoclinic cycles. *Physica* D **100** 85–100 (1997)

[19] M. Krupa. Robust heteroclinic cycles. *J. Nonlinear Science* **7** 129–176 (1997)

[20] I. Melbourne, P. Chossat and M. Golubitsky, Heteroclinic cycles involving periodic solutions in mode interactions with $\mathcal{O}(2)$ symmetry. *Proc. R. Soc. Edinburgh* **113A** 315–345 (1989)

[21] J. Swift, Hopf bifurcation with the symmetry of a square. *Nonlinearity* **1**, 333–377 (1988)

[22] E. Knobloch and M.R.E. Proctor, Nonlinear periodic convection in double-diffusive systems. *J. Fluid Mech.* **108** 291–316 (1981)

[23] E. Knobloch, On the degenerate Hopf bifurcation with $O(2)$ symmetry, in Multiparameter Bifurcation Theory (*Contemporary Math.* **56**) eds M. Golubitsky and J. Guckenheimer (AMS, Providence, RI) 193–201 (1986)

[24] J.W. Swift and E. Barany, Chaos in the Hopf bifurcation with tetrahedral symmetry: convection in a rotating fluid with low Prandtl number. *Eur. J. Mech. B/Fluids* **10** suppl. 99–104 (1991)

[25] G. Ahlers and K.M.S. Bajaj, Rayleigh-Bénard Convection with Rotation at Small Prandtl Numbers, *Proceedings of the IMA Workshop on 'Pattern Formation in Continuous and Coupled Systems'* eds M. Golubitsky, D. Luss, and S. Strogatz. Springer, (1999)

[26] J.H.P. Dawes, The transition between steady and oscillatory motion in three-dimensional rotating convection. *submitted to Physica D.*

[27] J.H.P. Dawes, Rapidly rotating thermal convection at low Prandtl number. *submitted to J. Fluid Mech.*

[28] J. Guckenheimer and P.J. Holmes, *Nonlinear oscillations, dynamical systems and bifurcations of vector fields.* Applied Mathematical Sciences Series, volume 42. Springer, New York, (1983)

[29] P.J. Holmes and D.A. Rand, Phase portraits and bifurcations of the nonlinear oscillator $\ddot{x} + (\alpha + \gamma x^2)\dot{x} + \beta x + \delta x^3 = 0$. *Int. J. Nonlinear Mech.* **15** 449–458 (1980)

[30] F. Takens, Forced oscillations and bifurcations. *Comm. Math. Inst., Rijkuniversiteit Utrecht* **3** 1–59 (1974)

[31] E. Knobloch and M. Silber, Oscillatory convection in a rotating layer. *Physica* D **63** 213–232 (1993)

[32] S.A. van Gils and M. Silber, On the uniqueness of invariant tori in $D_4 \times S^1$ symmetric systems. *Nonlinearity* **8** 615–628 (1995)

[33] B. Echebarria and H. Riecke, Instabilities of hexagonal patterns with broken chiral symmetry. *Physica* D **139** 97–108 (2000)

[34] M. Golubitsky and M. Roberts, A classification of degenerate Hopf bifurcations with $O(2)$ symmetry. *J. Diff. Eqns.* **69** 216–264 (1987)

[35] J.D. Crawford and E. Knobloch, Classification and unfolding of degenerate Hopf bifurcations with $O(2)$ symmetry: no distinguished parameter. *Physica* D **31**, 1–48 (1988)

Table 1
Solution branches in the Hopf bifurcation with $\mathbb{Z}_4 \ltimes T^2$ symmetry, fixed point subspaces and isotropy subgroups, reproduced from [13]. Stability criteria are only given for the first four solutions which are those guaranteed to exist by the Equivariant Hopf Theorem. Generically the SCR solution is unstable when it exists. The group elements are specified in the form $\rho^n[(\xi,\eta),\phi]$. A solution is stable when all quantities in the last column are negative. $f = a + b - c - d$ and a subscript r denotes 'the real part of'.

Name	Fix(Σ) (A_1, A_2, B_1, B_2)	Σ	Generators of Σ	Stability
TR	$(z,0,0,0)$	$S^1 \times SO(2)$	$[(\phi,\phi),\phi]$, $[(0,\phi),0]$	a_r, $b_r - a_r$, $c_r - a_r$, $d_r - a_r$
SR	$(z,z,0,0)$	$SO(2) \times \mathbb{Z}_2$	$[(0,\phi),0]$, ρ^2	$a_r + b_r$, $a_r - b_r$, $-f_r$, $\lvert e\rvert^2 - \lvert f\rvert^2$
SS	(z,z,z,z)	$\mathbb{Z}_4$	ρ	$a_r + b_r + c_r + d_r + e_r$, $a_r - b_r - e_r$, $f_r - 3e_r$, $Re(f\bar{e}) - \lvert e\rvert^2$
AR	$(z,z,\mathrm{i}z,\mathrm{i}z)$	$\tilde{\mathbb{Z}}_4$	$\rho[(0,\pi),\pi/2]$	$a_r + b_r + c_r + d_r - e_r$, $a_r - b_r + e_r$, $f_r + 3e_r$, $-Re(f\bar{e}) - \lvert e\rvert^2$
SCR	(z_1,z_1,z_2,z_2)	$\mathbb{Z}_2$	ρ^2	
TB	$(z_1,0,z_2,0)$	S^1	$[(\phi,\phi),\phi]$	

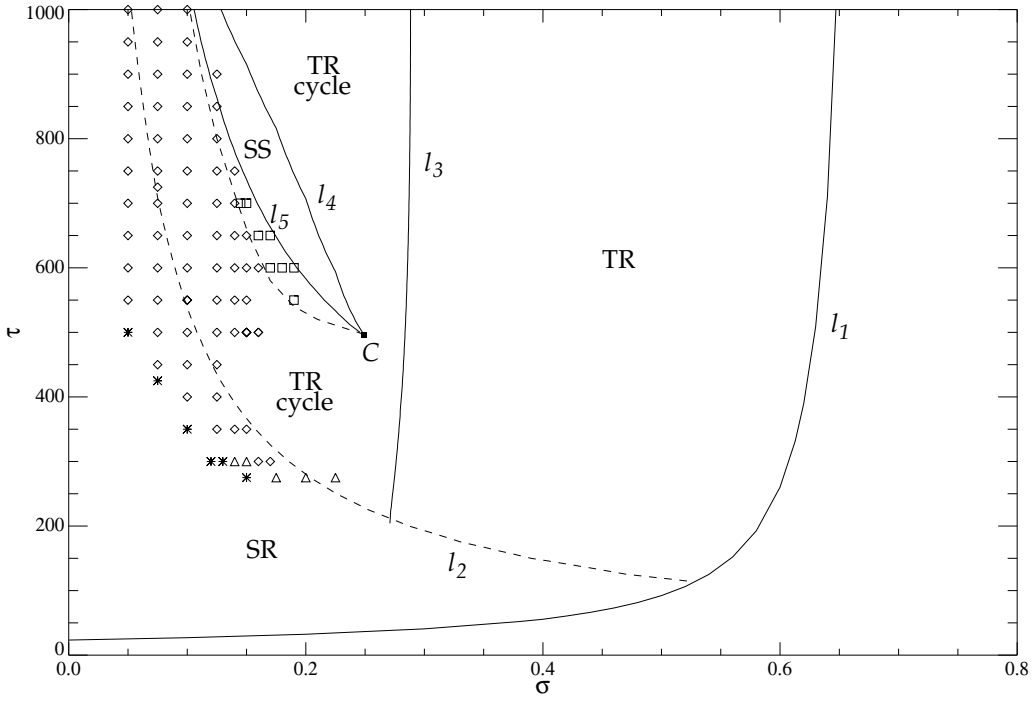

Fig. 1. Regions of the (σ,τ) plane where periodic solutions are stable. Other quasiperiodic and chaotic solutions are denoted by symbols: $\diamond$ - quasiperiodic solution near the heteroclinic cycle (see figure 3), $\triangle$ - triply-periodic solution, $*$ - chaotic solution (see figure 4), $\square$ - quasiperiodic solution within the SCR subspace. The dashed line ending at $\mathcal{C}$ gives the approximate location of the global bifurcation where the $\square$ solutions disappear.

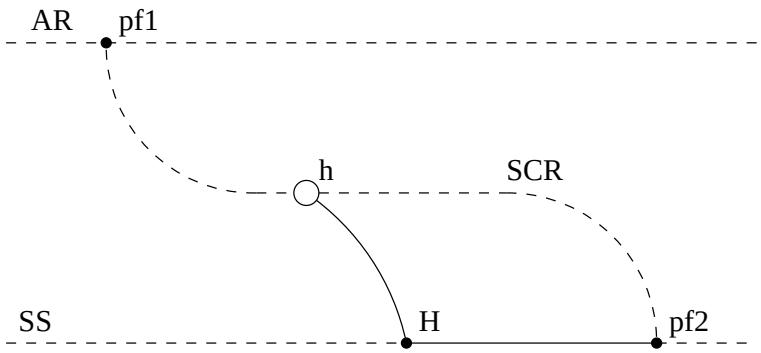

Fig. 2. Bifurcation behaviour in the normal form as σ increases (from left to right) on a line of constant $\tau = 525 > \tau^*$. $\sigma_{pf1} = 0.1064$, $\sigma_h = 0.2267$ (a point on the dashed line starting from $\mathcal{C}$ in figure 1), $\sigma_H = 0.2372$ (on ℓ_5 in figure 1), $\sigma_{pf2} = 0.2447$ (on ℓ_4 in figure 1). Solid (dashed) lines represent stable (unstable) solutions respectively. The quasiperiodic solutions existing for $\sigma_h < \sigma < \sigma_H$ are denoted $\square$ on figure 1.

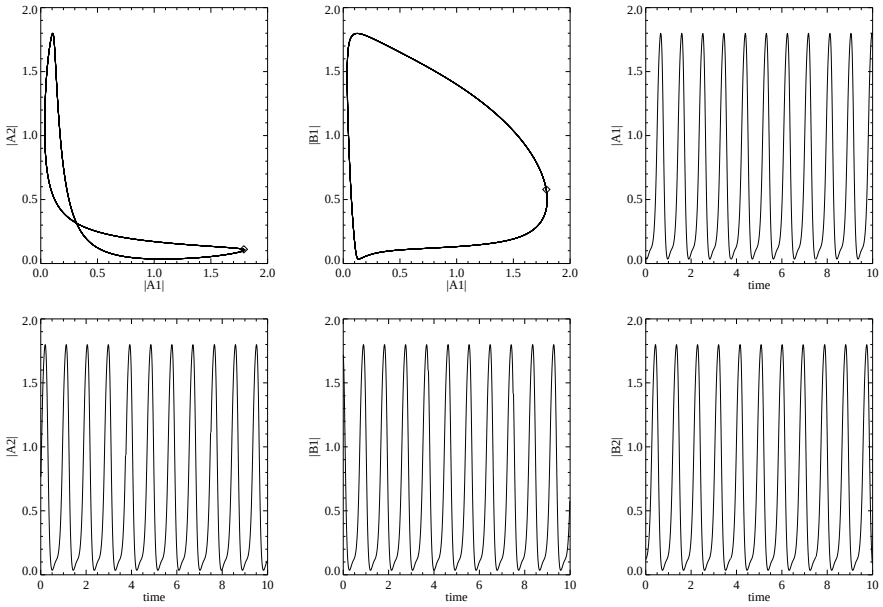

Fig. 3. An example of a quasiperiodic solution at $(\sigma, \tau) = (0.15, 350)$. Coefficients: $\mu = 5.0$, $a = -0.9264 + 0.7111\mathrm{i}$, $b = -0.8834 - 0.0808\mathrm{i}$, $c = -8.3930 - 2.5889\mathrm{i}$, $d = 1.9512 - 1.4475\mathrm{i}$, $e = -0.32681 - 3.0215\mathrm{i}$.

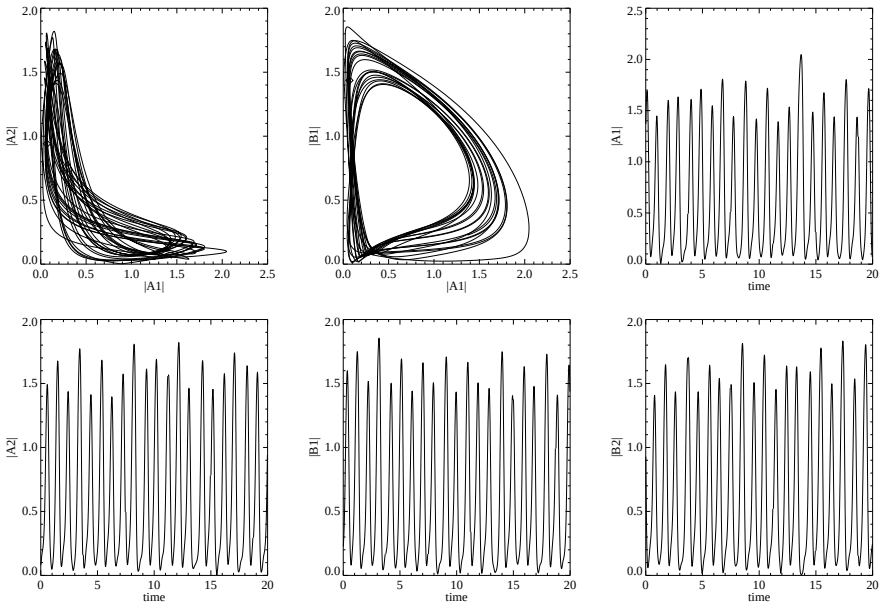

Fig. 4. An example of a chaotic solution at $(\sigma, \tau) = (0.15, 275)$. Coefficients: $\mu = 5.0$, $a = -1.0479 + 1.2076\mathrm{i}$, $b = -0.7108 + 0.0309\mathrm{i}$, $c = -7.6543 - 3.8686\mathrm{i}$, $d = 1.3770 - 1.8864\mathrm{i}$, $e = -1.0565 - 3.2504\mathrm{i}$.

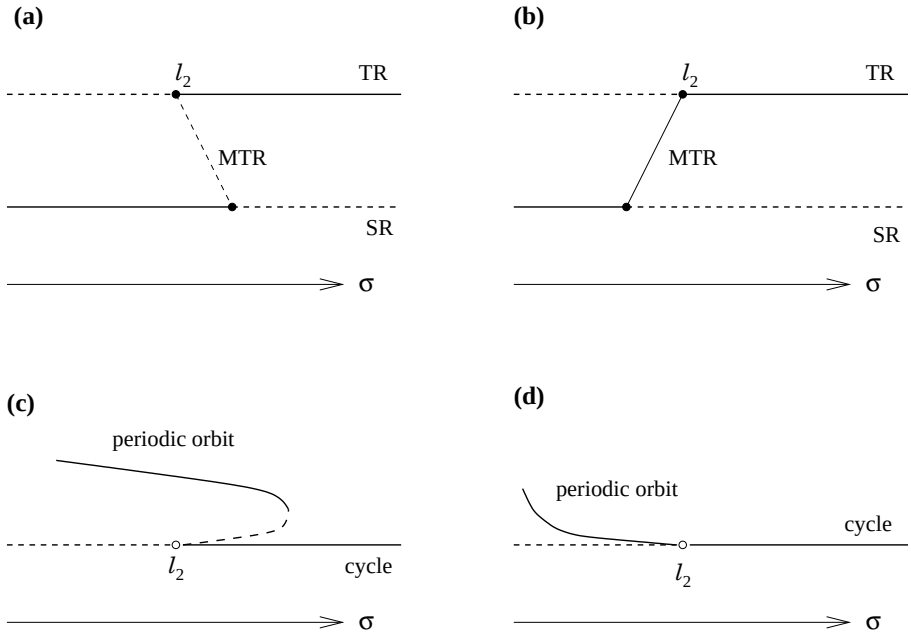

Fig. 5. Possible local and global bifurcation behaviour near ℓ_2 in figure 1. (a) and (b) show the two possible unfoldings of the degenerate situation $a_r - b_r = 0$; in (a) the Modulated Travelling Rolls (MTR) are unstable, and in (b) they are stable. (c) The global bifurcation when $|\Delta| > 1$: an unstable periodic orbit bifurcates subcritically. (d) The global bifurcation when $|\Delta| < 1$: a stable periodic orbit bifurcates supercritically.

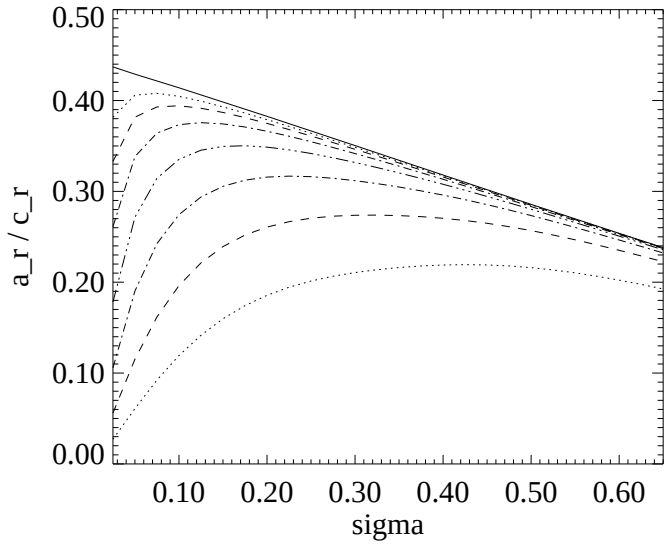

Fig. 6. Convergence of the ratio of normal form coefficients a_r/c_r as $\tau \to \infty$. From lowest upwards the lines are at constant values of τ: 10^4, 10^5, ..., 10^{10}. The solid straight line is the asymptotic behaviour obtained by Julien & Knobloch [12]. Note the very slow rate of convergence at low σ.

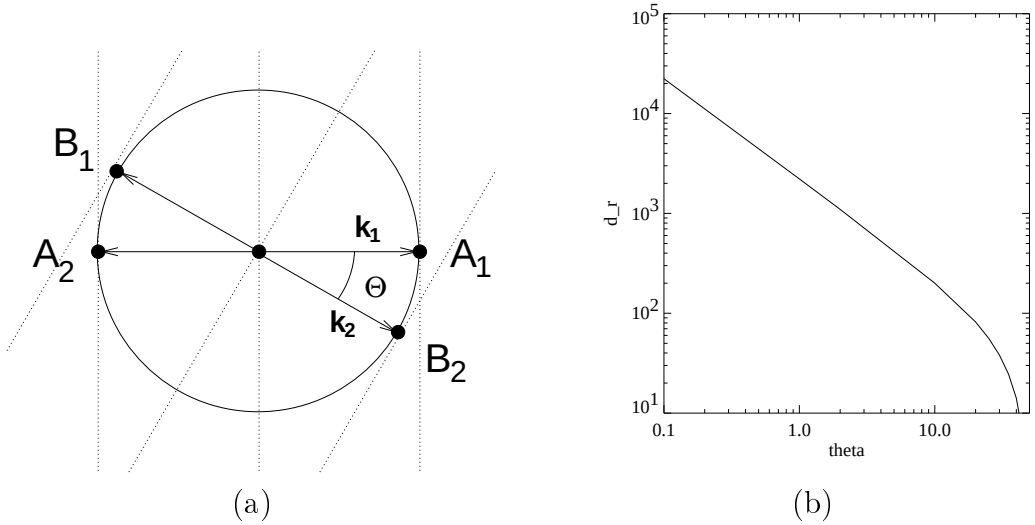

Fig. 7. (a) The marginal wavevectors $\mathbf{k_1}$ and $\mathbf{k_2}$ (solid lines) superimposed on the rhombic lattice (dotted lines). (b) The coefficient d_r as a function of the angle of the rhombic lattice Θ, measured in degrees, at $(\sigma, \tau) = (0.5, 500)$. For these parameter values the normal form coefficients calculated for a square lattice are $a = -4.420 - 5.163\mathrm{i}$, $b = -8.387 - 6.575\mathrm{i}$, $c = -46.07 - 1.391\mathrm{i}$, $d = -23.428 - 2.364\mathrm{i}$, $e = 27.639 - 7.334\mathrm{i}$.

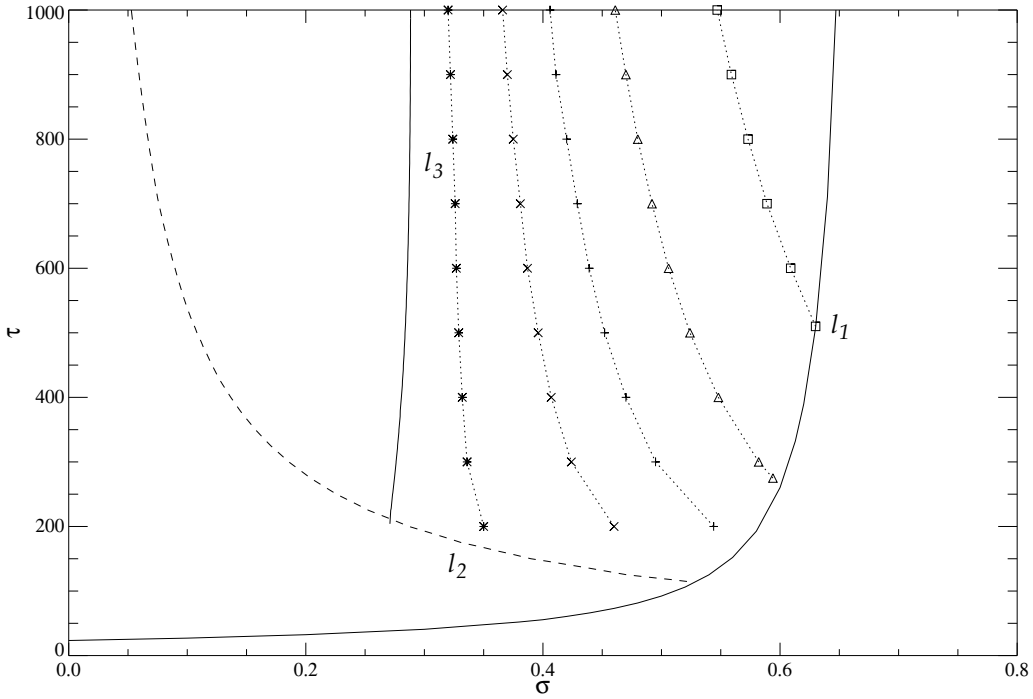

Fig. 8. The marginal stability of TR to inclined perturbations: to the right of the dotted lines, TR solutions are stable to perturbations at 80° - $*$; 70° - $\times$; 60° - $+$; 50° - $\triangle$; 40° - $\square$. Points are exact, dotted lines are guides to the eye.